JOURNAL OF Applied Polymer SCIENCE

# Crystal Polymorphism and Enhanced Dielectric Performance of Composite Nanofibers of Poly(vinylidene fluoride) with Silver Nanoparticles

**Naien Shi,[1] Juanjuan Duan,[1] Jie Su,[2] Fengzhen Huang,[2] Wei Xue,[1] Chao Zheng,[1] Yan Qian,[1] Shufen Chen,[1] Linghai Xie,[1] Wei Huang[1]**

[1]Key Laboratory for Organic Electronics and Information Displays, Institute of Advanced Materials, Nanjing University of Posts and Telecommunications, Nanjing 210046, People's Republic of China

[2]National Laboratory of Solid State Microstructures, Physics Department, Nanjing University, Nanjing 210093, People's Republic of China

Correspondence to: L. Xie (E-mail: iamlhxie@njupt.edu.cn) or W. Huang (E-mail: wei-huang@njupt.edu.cn)

**ABSTRACT:** Composite nanofibers of poly(vinylidene fluoride) ($PVF_2$) with silver nanoparticles are fabricated by electrospinning. According to the X-ray diffraction patterns and Fourier transform IR (FTIR) spectra, the content of piezoelectric $\beta$-polymorph of $PVF_2$ is enhanced in the composite fibers of $PVF_2$ and silver as compared with the pristine $PVF_2$ raw materials and electrospun nanofibers. The differential scanning calorimeter (DSC) measurement indicates that the composite of $PVF_2$ and silver has higher melting point and crystallization temperature than that of pristine $PVF_2$ nanofibers. Moreover, the existence of silver nanoparticles greatly enhances the dielectric constant of $PVF_2$ nanofibers and keeps a low dielectric loss simultaneously, which mainly relates to the internal fibrous structure of the composite. © 2012 Wiley Periodicals, Inc. J. Appl. Polym. Sci. 000: 000–000, 2012

**KEYWORDS:** electrospun nanocomposites; dielectric constant; crystal polymorphism

Received 11 April 2012; accepted 10 June 2012; published online
**DOI: 10.1002/app.38185**

## INTRODUCTION

Polymer nanocomposites have gained extensive attention in the past decade due to the improvement of the physical properties, such as higher moduli and improved thermal properties compared with the original polymer matrix.[1] Polymer-based materials with high dielectric permittivity are of great interest due to its potential applications in high charge storage capacitors,[2,3] spintronics,[4] and microelectromechanical systems,[5] organic printed circuit boards.[6–8] However, generally the dielectric constant of common polymers is too low (always 2–5), striving to substantially raise the dielectric constant of polymers have been an issue in the dielectric materials.[2,9]

Poly(vinylidene fluoride) ($PVF_2$) is a typical high-performance electroactive polymer with a high dielectric constant (generally 7–13 at 1 $\sim$ 1000 kHz).[9] Microscale ceramics and some other materials of high dielectric constant, such as $BaTiO_3$, ZnO, and CuPc, can be added to form a composite film to increase its dielectric constant, but higher loadings (generally more than 7 wt %) were necessary to achieve the high dielectric constant, which induced the problems of high weight, low flexibility, poor mechanical performance, and the agglomeration of the nanoparticles.[9–14] Conductive nanofillers such as carbon[9,15] or metallic materials[16,17] are also used as an additive to raise the dielectric constant by space charge polarization originating from the filler-conductor/polymer-insulator interfaces. However generally, the addition of conductive nanofillers enhances the dielectric constant of $PVF_2$ and causes a quite high dielectric loss simultaneously.[15–18] To ameliorate the dielectric behavior of polymer nanocomposites, a key issue is to enhance the dielectric constant of polymers, which reflects the ability of a material to store electric potential energy under the influence of an alternative electric field, and maintain the dielectric loss tangent which reflects the inherent dissipation of electromagnetic energy as low as possible.[5,6] Considering the polymorph and microstructure of polymers can heavily determine the electroactive properties of charge transport or storages,[19] we fabricated a polymer nanofibrous composite system consisting of $PVF_2$ nanofibers and silver nanoparticles by electrospinning. The silver nanoparticles in $PVF_2$ nanofibers were produced from the $AgNO_3$-$PVF_2$ nanofibers by *in-situ* reduction under light and were well-dispersed. Silver nanoparticle doped $PVF_2$ nanofibers were

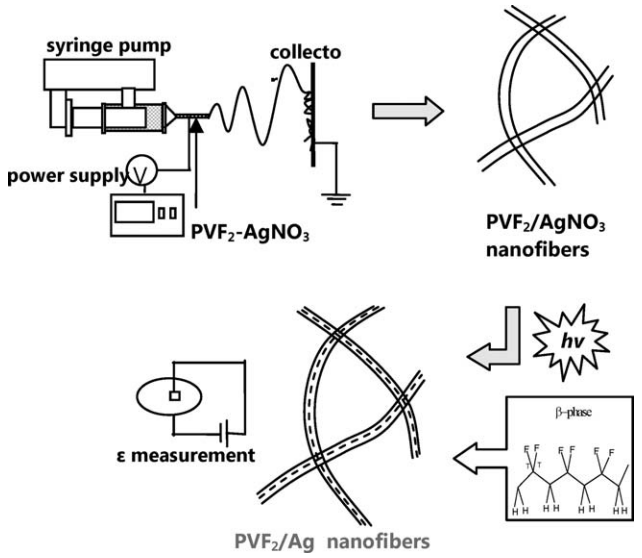


**Scheme 1.** Illustration of the electrospinning process for producing composite nanofibers of poly(vinylidene fluoride) with silver nanoparticles.

recently reported to serve as antibacterial materials.[20] Here we aim to utilize the intrinsic nanofibrous morphology to ameliorate the $PVF_2$ dielectric performance. We found that the pristine electrospun $PVF_2$ nanofibers have a dielectric constant of *ca.* 85 at 10 kHz. The composite $PVF_2$ nanofibers with silver nanoparticles induce an increment of the dielectric constant from 85 to 135, keeping a low dielectric loss as that of pristine $PVF_2$ nanofibers of about 0.03. Simultaneously, the thermal stability was enhanced and the piezoelectric polymorph was formulated in the composite.

## EXPERIMENTAL

### Materials

$PVF_2$ with $M_w = 120{,}000$ was provided by Si-Chuan Chenguang Research Institute in China and used without any further purification. Silver nitrate ($AgNO_3$, 99.8%) was purchased from Sinopharm Chemical Reagent, *N,N*-Dimethylformamide (DMF, 99.5%) and acetonitrile (99.0%) were purchased from Nanjing Chemical Reagent and used without any further purification.

### Preparation of the Nanofibers

DMF/acetonitrile mixed solution (v : v = 4 : 1, volume ratio) of $PVF_2$ at a concentration of 14% was obtained by continuously stirring at 35°C for 1 h to make it completely dissolved. The $AgNO_3$-$PVF_2$ solution was prepared by adding a small amount of solid $AgNO_3$ into the above DMF/acetonitrile solution of $PVF_2$ under vigorously stirring, and then the above fresh solutions were electrospun to obtain pristine $PVF_2$ and $AgNO_3$-$PVF_2$ composite nanofibers, respectively. The $AgNO_3$-$PVF_2$ composite nanofiber mat was left under sunny days for a week. The white composite nanofibers gradually changed to pale yellow. Different samples with $AgNO_3$ content of 0.058*M*, 0.03*M*, 0.02*M*, 0.01*M* (corresponding weight ratio of Ag:$PVF_2$ is 4.47%, 2.31%, 1.54%, 0.77%) were prepared, which was named as $PVF_2$-Ag-I, $PVF_2$-Ag-II, $PVF_2$-Ag-III, $PVF_2$-Ag-IV, respectively.

For the electrospinning process, first, the as-prepared solution was loaded into a standard 10-mL glass syringe. The open end of the syringe was attached to a blunt stainless steel hypodermic needle (OD = 0.9 mm), which was used as the nozzle. Whereas a piece of aluminum (Al) foil with ~ 15 cm in width was used as the collector. A High-Voltage DW-P403-1ACCC DC power supply was used to charge the solution by attaching the positive electrode to the nozzle and the negative grounding electrode to the aluminum collector. An electrical potential of 20 kV was applied across a distance of 10 cm between the needle tip and the collector, and a flow rate of 0.5 mL/h was employed. The electrospun fiber mats were collected over a period of 20 h.

### Characterization

SEM images were taken on a Hitachi S-4800 scanning electron microscope. TEM images were taken on a JEOL JEM-2100 transmission electron microscope. UV–vis absorption spectra of the samples were conducted at a Shimadzu UV3600-NIR-Recording spectrophotometer operated at resolution of 2 nm. FTIR spectra of the fibers were recorded on a Shimadzu IR Prestige-21 spectrophotometer as KBr pellets. XRD patterns were recorded on a Sweden ARL XTRA X-ray diffractometer with CuK$\alpha$ radiation ($\lambda = 1.5406$ Å). The samples were scanned in the range of 5–70° at room temperature. Differential scanning calorimeter measurement (DSC) was performed on a Shimadzu DSC-60A differential scanning calorimeter machine in the temperature range of 30 to 400°C at a scan rate of 10°C/min. The thermogravimetric analysis (TGA) of the samples was made using a Shimadzu DTG-60 instrument in the temperature range of 30–550°C at a heating rate of 10°C/min under $N_2$ atmosphere.

To measure the electrical properties of the films, the nanofibrous mat was removed from the aluminum foil, and pressed them into a disc with 13 mm in diameter and 0.8 ($\pm$0.1) mm in thickness under a pressure of $6.4*10^8$ Pa at room temperature. Silver dot electrodes were deposited onto the surface of the disc by vacuum evaporation through a shadow mask. The dielectric properties were evaluated using HP4194 impedance analyzer. Corresponding curves of dielectric constant and loss tangent vs. frequency are shown in Figure 8, which was recorded from 10 kHz.

## RESULTS AND DISCUSSION

After the obtained $PVF_2$/$AgNO_3$ electrospun nanofibers were left under sunny days, silver nitrate in the nanofibers decomposed to silver, nitrogen dioxide and oxygen,[21] and then the composite nanofibers of $PVF_2$ with silver nanoparticles were obtained (Scheme 1). Figure 1 shows the SEM images of pristine $PVF_2$ and silver-$PVF_2$ composite nanofibers. It can be seen that straight pristine $PVF_2$ nanofibers with 250 $\pm$ 100 nm in diameter [Figure 1(a,b)] and silver-$PVF_2$ composite nanofibers with 600 $\pm$ 200 nm in diameter [Figure 1(c,d)]. The TEM images shown in Figure 2 indicate that there are silver nanoparticles with 20–50 nm in diameter in the interior and on the surface of the $PVF_2$ nanofibers in the composite, as compared to the pristine $PVF_2$ nanofibers. Similar phenomenon was found in the nanofibers of silver nanoparticles doped $PVF_2$.[20] The

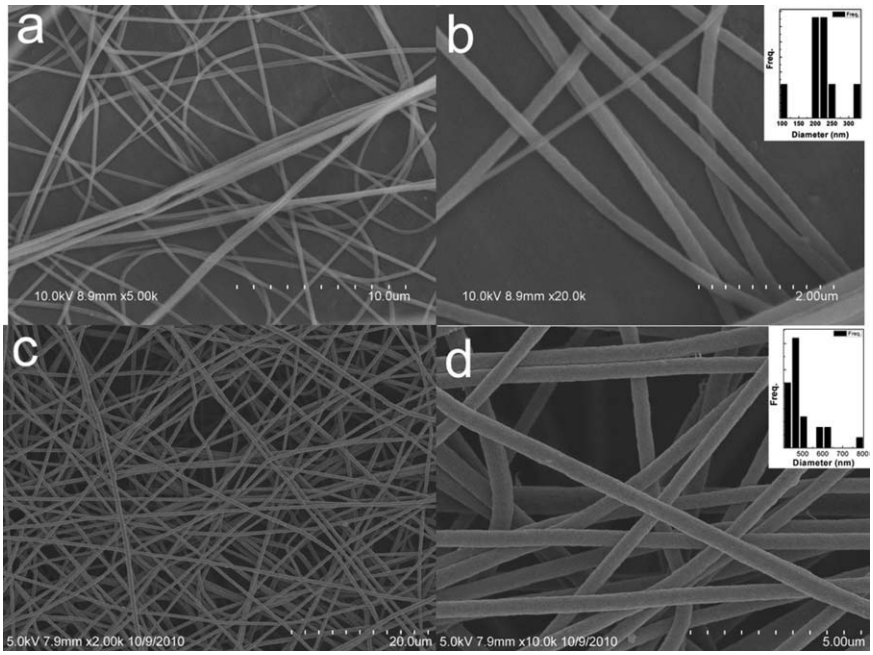


**Figure 1.** (a) and (b) Low and high magnification SEM images of pristine $PVF_2$ electrospun nanofibers. (c) and (d) Low and high magnification SEM images of $PVF_2$-Ag-I composite nanofibers. The inset shows the statistical result.

intimate encapsulation or absorption of the formed silver nanoparticles by $PVF_2$ benefits the difluoro methene/silver interaction between them. X-ray photoelectron spectroscopy (XPS) was performed to characterize the fine composition of the composite. Corresponding XPS spectrum shows that there are the elements of carbon, fluorine and silver [Figure 3(a)]. The binding energy of Ag $3d_{5/2}$ is 367.80 eV, which is different from protector-free silver nanoparticles (368.35 eV) [Figure 3(b)]. Since fluorine is a strong electronegative element, the $>CF_2$ dipole in $PVF_2$ may have affinity to the charges presented on the nanoparticle surface.[22] The negative shift was attributed to electrons in the difluoro methene donating to the 3d orbital of silver in the composite.[23,24] Corresponding energy dispersive spectrum also confirmed the existence of silver in the composite nanofibers [Figure 3(c)].

UV–vis absorption spectra of the electrospun fibers further confirmed the formation of silver nanoparticles (Figure 4). There is a broad band at about 410 nm which arises from the surface plasmon band of silver nanoparticles[22] in the spectra of silver-$PVF_2$ composite as compared with that of pristine $PVF_2$ nanofibers. With the increment of the silver content, the absorption intensity at longer wavelength of around 500 nm is enhanced, which may be attributed to the increment of the size of silver nanoparticles, or the different interparticle interaction and dielectric constant of the medium.[25–27]

As we know, there are five distinct crystal phases found in $PVF_2$: the nonpolar TGTG′ $\alpha$ and $\delta$ phase, the polar TTTT $\beta$ phase, and TTTGTTTG′ $\gamma$ and $\varepsilon$ phase, in which T and G are the trans and gauche chain conformations found in $PVF_2$ crystal.[1,28] The $\alpha$-polymorph is piezoelectrically inactive. However, the $\beta$-polymorph with all-trans chain conformation is orthorhombic and it is piezoelectrically active.[22,29] The $\gamma$-phase also has an orthorhombic unit cell, but it is piezoelectrically inactive.[22,30] The XRD patterns of the $PVF_2$ raw material, $PVF_2$ nanofibers and silver-$PVF_2$ composite nanofibers are shown in Figure 5. For the $PVF_2$ raw materials, there is a very strong peak at 20°, which corresponds to 200/110 reflections of the $\beta$-phase, and a shoulder peak at around 18°, which corresponds to 020 reflections of the $\alpha$-phase,[31] and a small broad peak at 35°, which corresponds to $\gamma$-phase.[28] These indicated the coexistence of the $\alpha$-, the $\beta$- and the $\gamma$-phase in the $PVF_2$ raw material. In the pristine $PVF_2$ electrospun nanofibers, the reflections of $\gamma$-phase disappeared and the shoulder peak at 18° for the $\alpha$-phase decreased obviously, which indicates that the electrospun process supports the transformation form TTTGTTTG′ $\gamma$- and TGTG′ $\alpha$-phase to TTTT piezoelectric $\beta$- polymorph. For the composite of $PVF_2$ with silver nanoparticles, the intensity of the reflections at 18° for the $\alpha$-phase further decreased, which was in accord with the result of the FTIR spectra shown in Figure 6, where the decrement of the intensity of $\alpha$-phase

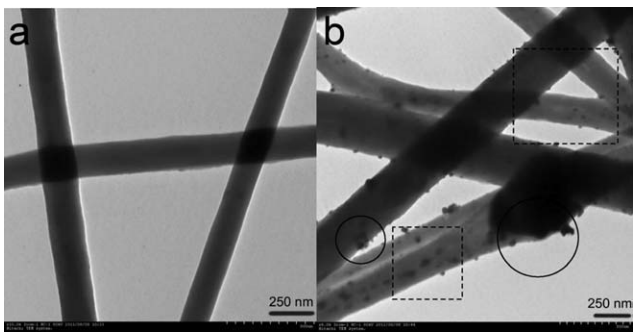


**Figure 2.** TEM images of (a) pristine $PVF_2$ nanofibers and (b) silver-$PVF_2$ composite nanofibers (the scale bar is 500 nm).

Applied Polymer SCIENCE

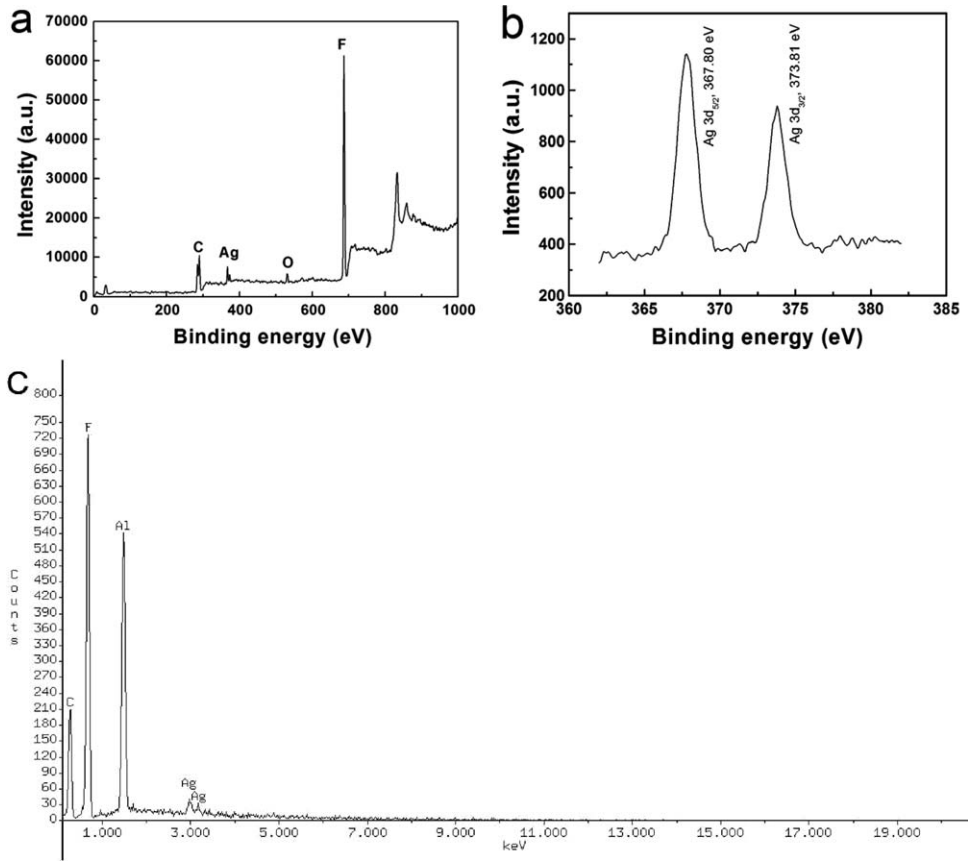


**Figure 3.** (a) and (b) XPS spectrum of the $PVF_2$-Ag-I composite nanofibers. (c) EDS of the $PVF_2$-Ag-I composite nanofibers.

related bands can be observed at 620, 769, and 796 $cm^{-1}$, while the containment of the $\beta$-phase related bands at 840 and 1278 $cm^{-1}$[30] in the composite. The peak at around 38° which gradually grows with the increasing concentration of silver arises from the metal of silver.[22,32] Silver nanoparticles can further induce the $PVF_2$ to crystallize in $\beta$-conformation, probably because the interaction of the $>CF_2$ dipole of $PVF_2$ with Ag nanoparticle induces the $-CH_2-CF_2$ unit to adopt an all trans conformation.[22]

The DSC thermograms and TGA curves of $PVF_2$ and the silver-$PVF_2$ composite for the heating and cooling processes are presented in Figure 7. It is obvious that the melting temperature of the $PVF_2$-Ag nanocomposite is increased as compared to that of pristine $PVF_2$ nanofibers, which is 133 and 128°C, respectively, although they have a similar glass transition temperature at about 119°C. The Ag nanoparticles influence the $PVF_2$ to

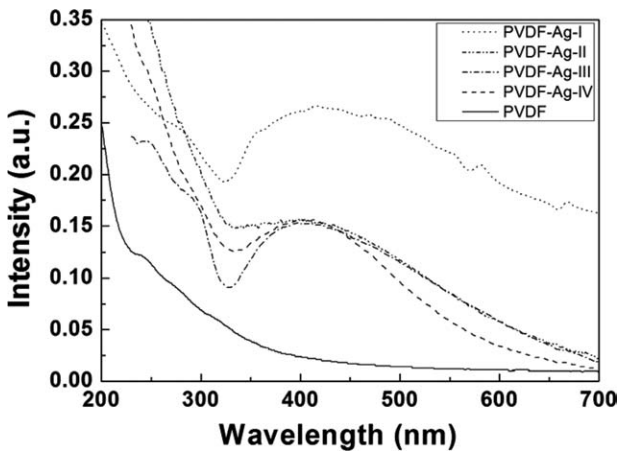


**Figure 4.** UV–vis absorption spectra of pristine $PVF_2$ nanofibers and composite nanofibers of $PVF_2$-Ag-I, $PVF_2$-Ag-II, $PVF_2$-Ag-III, $PVF_2$-Ag-IV.

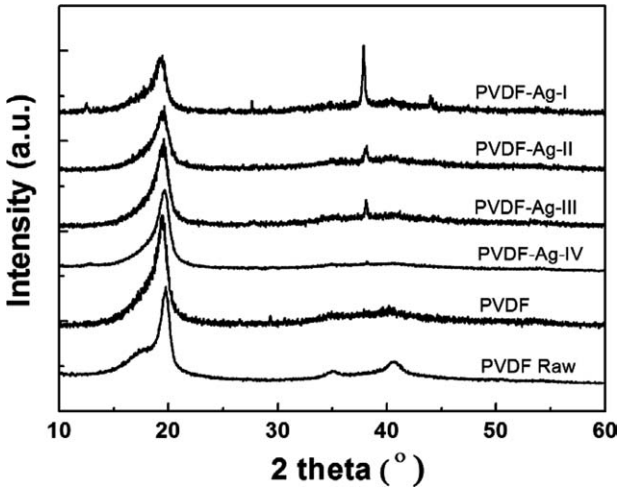


**Figure 5.** X-ray diffraction patterns of the pristine $PVF_2$ nanofibers and silver-$PVF_2$ composite nanofibers.

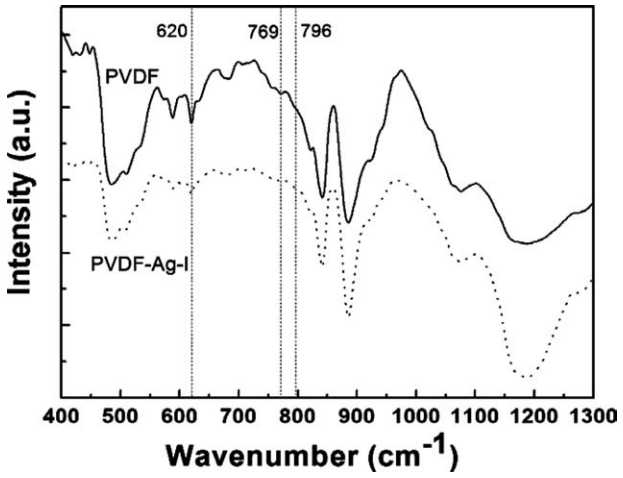


**Figure 6.** FTIR absorption spectra of the pristine $PVF_2$ nanofibers and silver-$PVF_2$ composite nanofibers.

crystallize in $\beta$-form, which has a higher melting point than that of the pristine $PVF_2$ nanofibers. Moreover, during the cooling process, the peak temperatures of the exotherms are 104 and 115°C for $PVF_2$ and the composite, respectively. This indicates that the $PVF_2$-Ag nanocomposite has a crystallization temperature higher than that of pure $PVF_2$, indicating that the Ag nanoparticles act as nucleating agents of $PVF_2$ crystallization in the composite.[22] Finally, their degradation temperature are 456 and 470°C, respectively. The above indicates that the thermal stability of pristine $PVF_2$ electrospun nanofibers was enhanced by the introduction of silver nanoparticles into the $PVF_2$ nanofibers.

The dielectric property of the electrospun $PVF_2$ and the composite of $PVF_2$ with silver nanoparticles were measured at room temperature, and the results are shown in Figure 8. It is seen that the dielectric constant of $PVF_2$ is greatly enhanced from 85 for the pristine nanofibers to 135 for the 0.01M ($PVF_2$-Ag-IV) composite nanofibers at the frequency of about 10 kHz, while low dielectric loss of about 0.03 are observed at the same frequency for both of the samples, which is much higher than the reported dielectric constant of $PVF_2$ film of 7–13.[14] In the $PVF_2$-silver composite, due to the electronegative feature of fluorine, it may generate large amounts of microcapacitors composed of the conductive silver nanoparticles and insulating $PVF_2$.[33] The enhancement of dielectric constant may arises from the interfacial space–charge polarization between the matrix of $PVF_2$ and the fillers of silver nanoparticles. The fibrous structures which maintained inside the pressed disc (Figure 9) should also benefit space-charge polarization and contribute to the enhancement of dielectric constant.[18] This can be deducted by the fact of the higher dielectric constant of 85 for the pristine $PVF_2$ fibers as compared with 7–13 for $PVF_2$ film. Normally, the addition of conductive fillers may caused a higher dielectric loss because of the piling charges at the extend interface.[32] However, the dielectric loss of our $PVF_2$-silver composites is very low and even less than that of pristine $PVF_2$. This may be attributed to two reasons. The first is that the produced silver nanoparticles in $PVF_2$ nanofibers by *in-situ* reduction are absorbed by the $>CF_2$ groups of $PVF_2$ via the affinity between the charges of the nanoparticles and $PVF_2$, and well dispersed in the nanofibrous composite (see the nanoparticles inside the dashed frames in Figure 2), so a continuous conductive network with high current leakage is difficult to form at the doping ratio in our experiment. The abnormal dielectric loss may be also attributed to the Coulomb blockade effect, the well-known quantum effect of metal nanoparticles, which reduces the electron tunneling.[34] Some recent studies reported that the porous polymer nanofibers exhibited a low dielectric performance.[35,36] Here the reversed enhanced dielectric performance of the pressed pellet of pure $PVF_2$ and its composite fibers in our experiment may be attributed to the exclusion of the air embedded in the pores.

Next, the dielectric constant decreased with the increasing content of silver nanoparticles and finally fell to 76 for the 0.058*M* ($PVF_2$-Ag-I) composite at the frequency of about 10 kHz. The decrement may arise from the growth of more silver nanoparticles and the interaction between the two components, which inclined to form a localized conductive network (see the aggregated nanoparticles inside the solid circles in Figure 2).[3] According to the percolation theory, the effective dielectric constant of the conductive-nanofiller/polymer-host composite increases with an increase in filler volume fractions and reaches its maximum at the percolation threshold, followed by a decrease with a further increase of filler volume fractions.[16] However, we got similar dielectric constant as $PVF_2$-Ag-IV

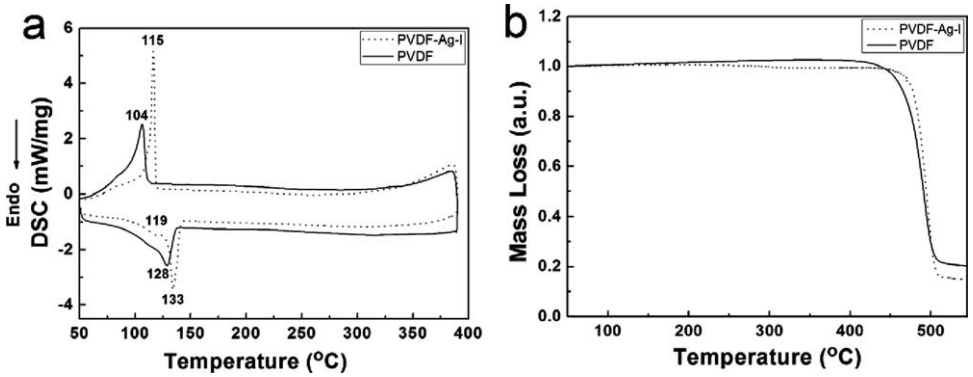


**Figure 7.** (a) DSC and (b) TG curves of pristine $PVF_2$ nanofibers and silver-$PVF_2$ composite nanofibers.

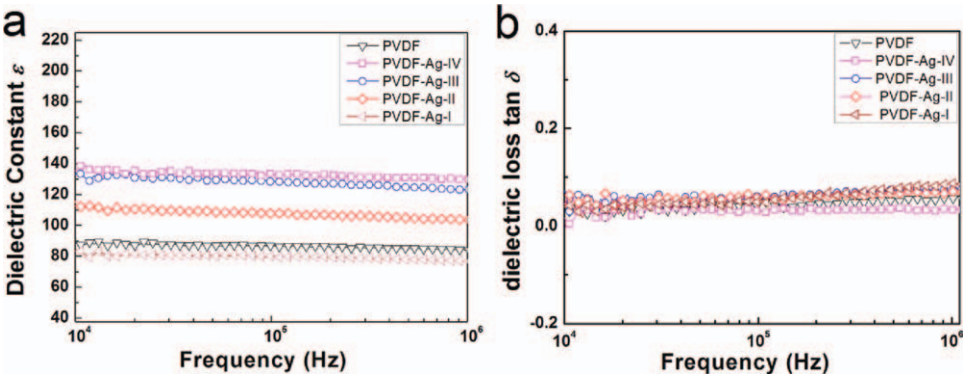


**Figure 8.** Dielectric constant (a) and loss (b) of electrospun pristine $PVF_2$ nanofibers and silver-$PVF_2$ composite nanofibers as a function of frequency at room temperature. [Color figure can be viewed in the online issue, which is available at wileyonlinelibrary.com.]

(0.01M) for the sample at one half concentration of $PVF_2$-Ag-IV (i.e. 0.005M, data not shown), so the dielectric constant of the samples here did not accord with the percolation theory which has been used to illustrate the dielectric constant change with the concentration of the fillers in many literatures.[14–17] This might relate to the fibrous microstructure of the samples and it is still under investigation. Finally, the dielectric constant of the reported $PVF_2$ composites generally decreased obviously with increasing the frequency, especially in the frequency range higher than 10 kHz, which is similar with the results of the composites with silver nanowires[16] and carbon nanofibers.[5,33] It is worth noting that the dielectric constant of the samples in this work shows a great frequency independence, for example, which changes only 4% in the frequency range of 10–1000 kHz for the $PVF_2$-Ag-IV composite (from 135 to 130).

## CONCLUSIONS

In summary, composite nanofibers of $PVF_2$ with silver nanoparticles are fabricated by electrospinning. Higher dielectric constant of about 135 and low dielectric loss of about 0.03 were observed for the 0.01*M* ($PVF_2$-Ag-IV) composite nanofibers at the frequency of about 10 kHz. Moreover, frequency independent dielectric constant was obtained for all the composite nanofibers, and the dielectric constant of these nanofibers can been tuned in the range of 135–76 by controlling the concentration of silver. The thermal stability of the $PVF_2$ composite nanofibers with silver nanoparticles was increased as compared with that of the pristine $PVF_2$ nanofibers. The obtained $\beta$-polymorph $PVF_2$ composite nanofibers may find potential applications in charge storage capacitors, microwave absorption, electromechanical systems, or antibacterial materials.

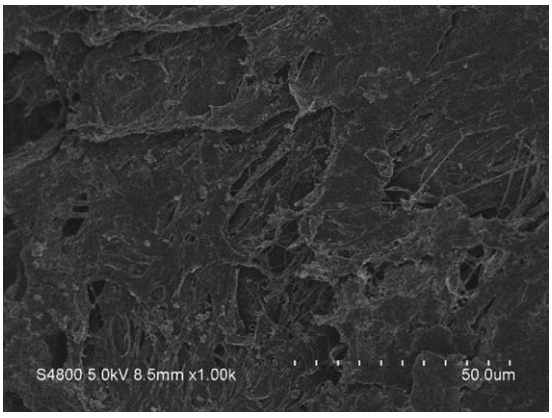


**Figure 9.** FESEM image of the transversal surface of $PVF_2$-Ag-IV composite nanofiber pressed disc for the dielectric measurement.

## ACKNOWLEDGMENTS

This work was financially supported by the Natural Science Foundation of the Education Committee of Jiangsu Province (10KJB510013, 11KJB510017), National Natural Science Foundation of China (21101095, 21144004, 61136003, 51173081, 21003076, 60907047) and the 973 Program of China (2009CB930600).

## REFERENCES

1. Yu, L.; Cebe, P. *Polymer* **2009,** *50*, 2133.
2. Yuan, J. K. S.; Yao, H.; Dang, Z. M. *J. Phys. Chem. C* **2011,** *115*, 5515.
3. Tomer, V. E.; Manias, C.; Randall, A. *J. Appl. Phys.* **2011,** *110*, 044107.
4. Lopez-Encarnacion, J. M.; Burton, J. D.; Tsymbal, E. Y.; Velev, J. P. *Nano. Lett.* **2011,** *11*, 599.
5. Sun, L. L.; Li, B.; Zhao, Y.; Mitchell, G.; Zhong, W. H. *Nanotechnology* **2010,** *21*, 305702.
6. Wang, C. H.; Hsieh, C. Y.; Hwang, J. C. *Adv. Mater.* **2011,** *23*, 1630.
7. Nguyen, T. T.; Tran, Q. H.; Seoul, Y. G.; Kim, D. I.; Lee, N. E. *ACS Nano* **2011,** *5*, 7069.
8. Lee, K. H.; Lee, K.; Oh, M. S.; Choi, J. M.; Im, S.; Jang, S.; Kim, E. *Organic Electronics* **2009,** *10*, 194.
9. Huang, X.; Jiang, P.; Kim, C.; Liu, F.; Yin, Y. *Eur. Poly. J.* **2009,** *45*, 377.
10. Chanmal, C. V.; Jog, J. P. *Exp. Polym. Lett.* **2008,** *2*, 294.
11. Li, K.; Wang, H.; Xiang, F.; Liu, W.; Yang, H. *Appl. Phys. Lett.* **2009,** *95*, 202904.
12. Devi, P. I.; Ramachandran, K. *J. Exp. Nanosci.* **2011,** *6*, 281.

13. Wang, J. W.; Wang, Y.; Wang, F.; Li, S. Q.; Xiao, J.; Shen, Q. D. *Polymer* **2009,** *50*, 679.
14. He, F.; Lau, S.; Chan, H. L.; Fan, J. *Adv. Mater.* **2009,** *21*, 710.
15. Li, Y. C.; Tjong, S. C.; Li, R. K. Y. *Syn. Met.* **2010,** *160*, 1912.
16. Zheng, W.; Lu, X. F.; Wang, W.; Wang, Z. J.; Song, M. X.; Wang, Y.; Wang, C. *Phys. Status Solidi A* **2010,** *207*, 1870.
17. Xu, H. P.; Xie, H. Q.; Yang, D. D.; Wu, Y. H.; Wang, J. R. *J. Appl. Polym. Sci.* **2011,** *122*, 3466.
18. Yuan, J. K.; Li, W. L.; Yao, S. H.; Lin, Y. Q.; Sylvestre, A.; Bai, J. *Appl. Phys. Lett.* **2011,** *98*, 032901.
19. Aleshin, A. N. *Adv. Mater.* **2006,** *18*, 17.
20. Yuan, J.; Geng, J.; Xing, Z.; Shen, J.; Kang, I.-K.; Byun, H. *J. Appl. Poly. Sci.* **2010,** *116*, 668.
21. Annadhasan, M.; Sankarbabu, V. R.; Naresh, R.; Umamaheswari, K.; Rajendiran, N. *Colloids Surf., B* **2012,** *96*, 14.
22. Manna, S.; Batabyal, S. K.; Nandi, A. K. *J. Phys. Chem. B* **2006,** *110*, 12318.
23. Zhang, P.; Shan, T. K. *Appl. Phys. Lett.* **2002,** *81*, 736.
24. Huang, Y. J.; Li, D.; Li, J. H. *Chem. Phys. Lett.* **2004,** *389*, 14.
25. Kamat, P. V. *J. Phys. Chem. B* **2002,** *106*, 7729.
26. Liz-Marzan, L. M. *Langmuir* **2006,** *22*, 32.
27. Singh, S. P.; Karmakar, B. *Plasmonics* **2011,** *6*, 457.
28. Lin, Y.; Yao, Y. Y.; Yang, X. Z.; Shen, L. M.; Li, R. X.; Wu, D. C. *Chin. J. Polym. Sci.* **2009,** *21*, 511.
29. Wang, T. T.; Herbert, J. M.; Glass, A. M. In the Applications of Ferroelectric Polymers; Blackie & Sons Ltd.: London, **1988.**
30. Li, J. J.; Meng, Q. J.; Li, W. J.; Zhang, Z. C. *J. Appl. Polym. Sci.* **2011,** *122*, 1659.
31. Yee, W. A.; Kotaki, M.; Liu, Y.; Lu, X. H. *Polymer* **2007,** *48*, 512.
32. Han, M.; Li, X.; Li, B. J.; Shi, N. E.; Chen, K. J.; Zhu, J. M.; Xu, Z. *J. Phys. Chem. C* **2008,** *112*, 17893.
33. Dang, Z. M.; Wang, L.; Yin, Y.; Zhang, Q.; Lei, Q. Q. *Adv. Mater.* **2007,** *19*, 852.
34. Lu, J. X.; Moon, K. S.; Xu, J. W.; Wong, C. P. *J. Mater. Chem.* **2006,** *16*, 1543.
35. Li, Y. X.; Lu, X. F.; Liu, X. C.; Zhang, C. C.; Li, X.; Zhang, W. J.; Wang, C. *Appl. Phys. A* **2010,** *100*, 207.
36. He, F.; Sarkar, M.; Lau, S.; Fan, J.; Chan, L. H. *Polym. Test.* **2011,** *30*, 436.